Effect of the non-dipole field on the seasonal variation of the geomagnetic Sq(Y)

Lin Tian[1], Aimin Du[2], Sheng Huang[3], Hao Luo[1], Wen-yao Xu[1], and Yasong S Ge[4]

[1]Institute of Geology and Geophysics, Chinese Academy of Sciences
[2]Institue of Geology and Geophysics, Chinese Academy of Sciences
[3]Key Laboratory of Earth and Planetary Physics, Institute of Geology and Geophysics, Chinese Academy of Sciences, Beijing 100029, China
[4]Institute of Geology and Geophysics

November 22, 2022

Abstract

Different timescales of the daily amplitude of the geomagnetic Y component during quiet period (Sq(Y)) over several solar cycles at 25 mid-low latitudes observatories were analyzed. The annual mean (Sq_0), annual (Sq_1) and semiannual (Sq_2) components were separated from Sq(Y) by means of Fourier analysis method. No obvious distinction is found for the morphology of the spatial distribution of these Sq(Y) components during solar quiet and active periods, except that they are more intense in high solar activity. Sq_1(Y) exhibits a remarkable longitudinal inequality, which is much stronger around Eurasia and Australia anomaly zones and weaker around South Atlantic Ocean anomaly zones. The positive correlation between Sq_0(Y) and geomagnetic vertical component Z suggests that the convection electric fields in the dynamo region play a key role in controlling annual mean (Sq_0). On the other hand, the Sq_1(Y) exhibits a positive correlation with geomagnetic horizontal component H, implying the inter-hemispheric field-aligned currents (IHFACs) may contribute to difference of the annual variation amplitude at different observatories. The Sq_2(Y) is most prominent in the South Atlantic Ocean anomaly (SAO) region. It is possible the stronger ionospheric conductivity in the dynamo region contribute to the remarkable semiannual variation at SAO region.

Effect of the non-dipole field on the seasonal variation of the geomagnetic Sq(Y)

Lin Tian[1, 2], Aimin Du[1, 2, *], Sheng Huang[1], Hao Luo[1, 2, *], Wenyao Xu[1, 2], Yasong Ge[1, 2]

[1]Key Laboratory of Earth and Planetary Physics, Institute of Geology and Geophysics, Chinese Academy of Sciences, Beijing 100029, China;

[2]College of Earth Science, University of Chinese Academy of Sciences, Beijing, China

Corresponding author: Hao Luo (luohao06@gmail.com); Aimin Du (amdu@mail.igcas.ac.cn)

Key points:

1. The Sq(Y) at 25 mid-low observatories were statistically investigated by decomposing into different timescales.
2. Annual mean, annual variations, and semiannual variations were analyzed with respect to the geomagnetic components.
3. The non-dipole filed has strong effects on Sq(Y) with different timescales.

Abstract. Different timescales of the daily amplitude of the geomagnetic Y component during quiet period (Sq(Y)) over several solar cycles at 25 mid-low latitudes observatories were analyzed. The annual mean (Sq_0), annual (Sq_1) and semiannual (Sq_2) components were separated from Sq(Y) by means of Fourier analysis method. No obvious distinction is found for the morphology of the spatial distribution of these Sq(Y) components during solar quiet and active periods, except that they are more intense in high solar activity. Sq$_1$(Y) exhibits a remarkable longitudinal inequality, which is much stronger around Eurasia and Australia anomaly zones and weaker around South Atlantic Ocean anomaly (SAO) zones. The positive correlation between Sq$_0$(Y) and geomagnetic vertical component *Z* suggests that the convection electric fields in the dynamo region play a key role in controlling annual mean (Sq$_0$). On the other hand, the Sq$_1$(Y) exhibits a positive correlation with geomagnetic horizontal component *H*, implying the inter-hemispheric field-aligned currents (IHFACs) may contribute to difference of the annual variation amplitude at different observatories. The Sq$_2$(Y) is most prominent in the SAO region. It is possible the stronger ionospheric conductivity in the dynamo region contribute to the remarkable semiannual variation in SAO region.

1. Introduction

It is well known that the solar quiet daily geomagnetic variation (Sq) at mid-low latitudes primarily originated from the dayside ionospheric E-region dynamo [Matsushita, 1967; Forbes and Lindzen, 1976; Richmond, 1979; Yamazaki et al., 2017]. According to the classical dynamo theory, the distribution of the Earth's main field in space, the tidal wind, and the ionospheric conductivity control the behavior of the Sq type variation [Campbell, 1982]. In particular, the geomagnetic field not only modulates the conductivity through its dependence on the electron and ion gyrofrequencies, but also controls the dynamo electric field [Stening, 1971; Takeda, 1996; Le Sager and Huang, 2002]. As a consequence of these factors, the Sq electric current systems show a remarkable dependence on season, solar activity, longitudinal zone and hemisphere [*Matsushita and Maeda*, 1965; Campbell, 1982; Takeda, 1999, 2002a; Pedatella et al., 2011; Yamazaki et al., 2011].

The seasonal variation of Sq is identified by the ground-based [Currie, 1966; Banks and Nullard, 1966; Wagner, 1969; Bhargava, 1972; Campbell, 1982; Takeda, 1999; 2002a; Yamazaki et al., 2009] and satellite magnetometers [e.g. sPedatella et al., 2011]. The Sq intensity shows a conspicuous annual variation at each hemisphere [e.g., Matsushita and Maeda, 1965; Takeda, 2002a]. It enhances during the local summer and decreases during the local winter. This is consistent with the annual change of the insolation and E-region ionization level [Yamazaki et al., 2009]. A distinct semiannual variation of the Sq intensity with maxima near the equinoxes and minima near the solstices is also found [*Campbell and Matsushita*, 1982; Hibberd, 1985; Stening, 1995; Takeda, 1999, 2002a; Pedatella et al., 2011], however its incidence varies with hemisphere, longitude and local time [Stening, 1995]. In contrast, the seasonal variation of the foci of the Sq current system is more complicated. Typically, the foci are located between 30^{o} and 35^{o} dip latitudes [Matsushita and Maeda 1965]. Previous studies suggested that the northern foci moved poleward notably during September-November and the southern foci moved equatorward during January-February [Hasegawa, 1965; Tarpley, 1973; Stening et al, 2007]. Such foci shift in position is generally accompanied with the variation of the electrojet amplitude at the equator and could be associated with the variations in the tidal winds in the ionosphere [Campbell, 1982; Stening and Reztsova, 2005; Stening et al., 2007].

The influence of solar activity on Sq has also been studied for decades [e.g., Chapman and Bartels, 1940; Chapman et al., 1971; Rastogi and Iyer, 1976; Campbell and Matsushita, 1982; Briggs, 1984; Takeda et al., 1986; Takeda, 2002b, 2013a, b]. When the sunspot number (SSN) increases, the Sq amplitude enhances along with the increasing height integrated Pedersen and Hall conductivities in the ionosphere [Rastogi and Iyer, 1976; Briggs, 1984; Takeda, 2002b, 2013a]. The Sq current in the solar active year is about 1.6 to 3.0 times as large as that in the solar quiet year with the larger ratio occurring in mid-November [Campbell and Matsushita, 1982]. The seasonal change of the Sq varies with solar activity level as well [Chapman et al., 1971; Takeda, 2013a]. Campbell and Matsushita [1982] compared the Sq behavior in North American zones during solar active and quiet periods. They found that the Sq amplitude showed a dominant annual variation in the quiet year and a dominant semiannual variation in the active year. The semiannual variation was also conspicuous for sum of the northern and southern current intensities with maximum at April and at October or November in solar maximum years [Takeda, 1999, 2002a]. Since the relative amplitude of semiannual variation in Sq is much higher than that for the ionospheric conductivity, it is impossible to explain the semiannual variation of Sq intensity without taking into account other processes independent on the conductivity [Wagner et al., 1980; Yamazaki et al., 2009].

It is demonstrated that the Sq current whorls with the focus at the mid latitude is rather stable, regardless of the solar-terrestrial conditions [Campbell and Matsushita, 1982; Yamazaki et al, 2011]. Thus, the geomagnetic Y components at the mid-low latitude are reflected by equatorward current in the morning side and poleward current in the afternoon side. Takeda [2013a] analyzed the daily variation of the geomagnetic Y component (Sq(Y)) in several long-term operated observatories and found an obvious seasonal variation of Sq(Y), strongly dependent on the solar activity. Furthermore, the strength of the seasonal variation of Sq(Y) varies with its geographic location [Takeda, 2013a; 2013b]. The longitudinal inequalities in the Sq current system and its seasonal variation were also identified by the CHAMP satellite magnetic field observations [Pedatella et al., 2011]. By means of spherical harmonics analysis (SHA), Matsushita and Maeda [1965] revealed the features of the Sq current system in Asia-Australia, Europe-Africa and America Sectors and suggested the longitudinal variability was caused by the differences of the relative position of the geomagnetic and the geographic equators. Modeling results also clearly showed a strong dependence of the Sq current system on the longitudinal variation of the geomagnetic field [Stening, 1971; Le Sager and Huang, 2002].

Although there is no doubt that the geomagnetic field plays an important part in generating longitudinal variations in the Sq current system [Stening, 1971; Pedatella et al., 2011], the effects of the magnetic fields, especially the non-dipole field parts on the longitudinal and variabilities of Sq with different timescales remains an open question. A detailed investigation on seasonal variations of Sq in non-dipole geomagnetic anomaly, which strongly distorts the morphology of the geomagnetic dipole field, is very helpful for understanding the effect of the geomagnetic field on Sq. In this study, we examine the spatial distribution of seasonal variations of Sq(Y) in mid-low latitudes, and discuss its correlation with the geomagnetic field.

2. Data analysis

The one-hour geomagnetic data analyzed in this work are obtained at 25 mid-low latitude stations from World Data Center for Geomagnetism, Edinburgh (http://www.wdc.bgs.ac.uk/catalog/master.html). Table 1 lists the names and the geographic and geomagnetic coordinates of these stations and **Figure 1** shows the geographic distribution of them. Although the longitudinal distribution is quite inhomogeneous, the stations cover most longitudinal zones in both hemispheres. All stations have operated for at least one solar cycle and 80% of them provide available data for more than 20 years (listed in Table 1).

To avoid the effect of the magnetic disturbance, the geomagnetic data were selected in days (in local time) when the maximum of the geomagnetic disturbance index Kp is no more than 2+. In consideration of the day-to-day variability in the Sq geomagnetic field [Stening and Reztsova, 2005; Chen, et al, 2007], one-hour values of the geomagnetic data at each local time were averaged over a month to produce the monthly mean data.

In general, the geomagnetic horizontal components H have very different behavior for different longitudinal sectors in equinoctial months, with a positive peak around noon in the Asian and African sectors, but with a negative peak around noon in the American sector [Matsushita and Maeda, 1965; Campbell, 1989; Le Sager and

Huang, 2002]. In contrast, for *Y* components, it is relatively regular without large longitudinal phase changes. Thus, the monthly mean one-hour values of the geomagnetic *Y* component were chosen to investigate their seasonal variations in the present study. The daily variation of *Y* (Sq(Y)) is obtained as the difference between the maximum value in the morning (afternoon) side and the minimum value in the afternoon (morning) side in the northern (southern) hemisphere in the daytime [Takeda, 2002b, 2003a, b; Takeda et al., 2003]. The averaged horizontal and vertical components of the geomagnetic data in nocturnal intervals (0-1 LT) were calculated as a proxy of the geomagnetic main field at each station.

In consideration of intensive influence of the solar activity on Sq field, we made a comparison of Sq(Y) in the high and low solar activity state. Three maximum and minimum sunspot number years in each solar cycle were classified as higher and lower solar activity years. As shown in **Figure 2**, the high solar activity years show large variations in sunspot number (SSN) and Sq(Y) from one solar maximum to another (red dots). Since Sq(Y) has a pronounced linear dependence on monthly mean SSN, we normalized Sq(Y) to SSN=150 and SSN=20 for high and low solar activity years, relying on the linear relationship between Sq(Y) and SSN.

2.1 Spatial distribution of seasonal variations of Sq(Y)

Figure 3 shows the variations of Sq(Y) at KNY(130.9^{o}E, 31.4^{o}N) and CTA (146.3^{o}E, 20.1^{o}S) in Asia-Australia sector (**Figures 3a, 3b**), at TAM (5.5^{o}E, 22.8^{o}N) and TSU (17.6^{o}E, 19.2^{o}S) in Europe-Africa sector (**Figures 3c, 3d**), and at SJG (66.2^{o}W, 18.1^{o}N) and PIL (63.9^{o}W, 31.7^{o}S) in America sector (**Figures 3e, 3f**) in the northern hemisphere (left column) and the southern hemisphere (right column), respectively. It is noted that a similar semiannual or annual variation in Sq(Y) at one station is shown in **Figure 3** for both solar maximum and minimum years. The amplitude of Sq(Y) in the higher solar maximum years (red triangles) is about 40% more intensive than that in solar minimum years (blue diamonds) in the three sectors.

For northern hemispheric stations, the Sq(Y) enhances in March and declines in October, and no apparent amplitude dip appears in June solstices. These observational characteristics indicate the coupling of an annual variation with a peak of June and a semiannual variation with two peaks of March and September. The annual variations are larger than the semiannual variations in the northern hemisphere. The amplitudes of annual variations are strongest in KNY and weakest in SJG. The annual characteristics of Sq(Y) are in agreement with the observations by Rastogi et al. [1994] in Indian region and by Yamazaki et al. [2009] in 210^{o} magnetic meridian (MM) chain.

By contrast, the semiannual variations are prominent for stations in the southern hemisphere. The peaks of the seasonal variation appear in February and October in CTA station. The semiannual variations significantly enhance and play an important role in the African and South American zones (**Figures 3d, 3f**). However, it is clearly noted that the annual variation is also strong at CTA in the Australian zone (**Figure 3b**). The ground-based magnetometers and CHAMP satellite magnetometers have revealed that the seasonal variation in the Europe-Africa longitudinal sector of the southern hemisphere exhibits a primarily semiannual oscillation with maxima near equinoxes [Pedatella et al., 2011]. It also can explain the controversy of observations by Campbell and Matsushita [1982] and Stening [1995]. Campbell and Matsushita [1982] using data from North America stations noted that the semiannual Sq variation is distinct only during solar maximum period. However, Stening [1995] using data from global stations reported the semiannual Sq variation even during solar minimum period. One of the reasons causing the diversity of seasonal variation during maximum and minimum period is the dependence of semiannual variation of the strength of Sq(Y) on the geographic location.

We use Fourier harmonic analysis method [referring to Campbell, 1989] to separate the annual and semiannual variations from Sq(Y) for 25 stations. 12 monthly mean values of Sq(Y) averaged over all the low (or high) solar activity years were used to compute the Fourier harmonic components. The first three Fourier harmonics roughly represent the variations with periods of ~0, 1, and 0.5 years, respectively. We sign them as the stationary component, $Sq_0(Y)$, annual component, $Sq_1(Y)$, and semiannual component, $Sq_2(Y)$, respectively. The synthesis of the first three Fourier harmonic is in good agreement with the observed data (not shown in this paper).

Figure 4 shows the longitudinal distribution of $Sq_1(Y)$ and $Sq_2(Y)$ in the northern (left panels) and southern (right panels) hemispheres. In the northern hemisphere, the annual component $Sq_1(Y)$ is quite strong in the Asian sector (red line) and very weak in the North American sector (blue line). In contrast, the semiannual component $Sq_2(Y)$ for most northern stations are not so strong as Sq1(Y) both in solar quiet and active periods. The approximately equal values of Sq1(Y) and Sq2(Y) in North

American stations indicate the existence of the semiannual variation previously reported [*Campbell and Matsushita*, 1982].

In the southern hemisphere, the annual variation of $Sq_1(Y)$ is prominent in the Australian sector (red line), while much weaker in the African sector (blue line). $Sq_2(Y)$ is strong in the Australian and African stations and quiet weak in the Pacific stations. Notably, $Sq_2(Y)$ around the South Atlantic anomaly zone, such as the African station TSU and the South American station PIL, is extremely intense compared to $Sq_1(Y)$, indicating that the semiannual variation dominate in this zone.

Figure 5 shows the latitudinal distribution of $Sq_1(Y)$ and $Sq_2(Y)$ in the Asia-Australia sector (left panels) and the Europe-Africa sector (right panels). In the Asia-Australia sector, the annual component $Sq_1(Y)$ shows no obvious difference between the two hemispheres, and is slightly weaker in the equatorward station. $Sq_2(Y)$ in the northern hemispheric station is quiet weak in the solar quiet period, and becomes intense in the solar active period, as well as the Australian station PMG. In the Europe-Africa sector, asymmetric distribution of $Sq_1(Y)$ and $Sq_2(Y)$ between the two hemispheres is clearly demonstrated. $Sq_1(Y)$ in the southern hemisphere is much weaker than that in the northern hemisphere. On the contrary, $Sq_2(Y)$ in the southern hemispheric station are fairly strong in both the solar quiet and active periods, while $Sq_2(Y)$ in the northern hemispheric stations TAM and MBO are still quite weak.

2.2 Correlation of Sq(Y) with the geographic latitude and components of the geomagnetic field

Figure 6 depicts the correlation of $Sq_0(Y)$ with the geographic latitude, φ, and horizontal component, H, and vertical component, Z, of the geomagnetic field for northern (left column) and southern (right column) hemispheres. The stationary component $Sq_0(Y)$ enhances with increasing φ and Z for both high and low solar activity years. It is surprising that $Sq_0(Y)$ increases with decreasing of H. The slope of the linear fit during high solar activity years is generally larger than during low solar activity years.

The annual component $Sq_1(Y)$ exhibits a significantly different relationship with the geographic latitude and the geomagnetic components (shown in **Figure 7**). $Sq_1(Y)$ increases with increasing φ in the northern hemisphere, while reverses in the southern hemisphere. Instead, a better correlation between $Sq_1(Y)$ and H was found in both hemispheres (**Figures 7c and 7d**). Notably, the slope for the northern hemisphere was steeper than that for the southern hemisphere both in low and high solar activity. No obvious correlation between $Sq_1(Y)$ and the vertical component Z is found in both hemispheres.

The correlation of the semiannual component $Sq_2(Y)$ with the geographic latitude and the geomagnetic components is quite different in northern and southern hemispheres (shown in **Figure 8**). In the northern hemisphere, $Sq_2(Y)$ is rather small in solar quiet condition, and shows no significant correlations with the geographic latitude and H. Only a slight positive correlation between $Sq_2(Y)$ and Z is detected. In the high solar activity, $Sq_2(Y)$ is positively relevant to φ and H. In the southern hemisphere, $Sq_2(Y)$ becomes weaker in the lower latitude (**Figure 8b**) and intensifies as the geomagnetic component H decreases (**Figure 8d**), in spite of the solar-terrestrial condition. Similar to $Sq_1(Y)$, no distinct correlation with Z was found for $Sq_2(Y)$.

The correlation coefficients between Sq(Y) and the geographic latitude and components of the geomagnetic field are listed in Table 2. It suggests that the stationary component $Sq_0(Y)$ is significantly correlated with the geomagnetic vertical component Z and the annual component $Sq_1(Y)$ is significantly correlated with the geomagnetic horizontal component H. $Sq_2(Y)$ in the northern hemisphere shows no significant correlation with the geographic latitude and the geomagnetic field. In contrast, $Sq_2(Y)$ in the southern hemisphere correlated well with the geographic latitude and H. Additionally, $Sq_0(Y)$ in the northern hemisphere also shows a prominent relationship with the geographic latitude.

3. Discussions and Conclusions

It is well known that the geomagnetic non-dipole field zones are five large-scale anomalies (Xu and Bai, 2009), which are listed according to their maximum intensities as follows: the South Atlantic Ocean anomaly (SAO), Africa anomaly (AFR), Eurasia anomaly (ERA), Australia anomaly (AST), and North America anomaly (NAM). In particular, the two strongest negative anomalies (defined in total intensity) SAO and AFR dramatically distort the morphology of the geomagnetic field in the African sector as shown in **Figure 1**. In these African stations, Sq(Y) shows distinctive seasonal variations as well, where the semiannual variation is dominant both in the solar active and quiet periods.

Many studies have demonstrated that the geomagnetic field plays a key role in generating longitudinal variations in the Sq current system [Stening, 1977; Pedatella et al., 2011]. Pedatella et al. [2011] took into account the influence of non-migrating tides to account for the longitudinal variability. In our study, we compared the correlation between the seasonal components of Sq(Y) and the geomagnetic field components. It provides another way to investigate the cause of the longitudinal variability of Sq.

According to the classic dynamo theory, the geomagnetic main field controls the convection electric field of the Sq dynamo [Stening, 1971]. Weakening of the magnetic field decreases the electrostatic potential difference and increases the height-integrated ionospheric Pederson and Hall conductivity [Takeda, 1996]. Hence, the positive correlation between $Sq_0(Y)$ and the geomagnetic vertical component Z suggests that the ascending Z increases $Sq_0(Y)$ monotonously by means of enhancing the electrostatic potential. The negative correlation between $Sq_0(Y)$ and the geomagnetic horizontal component H implies that H affects $Sq_0(Y)$ by virtue of altering the ionospheric conductivity. In fact, the correlation coefficients between $Sq_0(Y)$ and Z are 0.83/0.81 in the northern/southern hemisphere during solar maximum, whereas those between $Sq_0(Y)$ and H are 0.49/0.36, indicating that $Sq_0(Y)$ significantly correlates with Z and insignificantly correlates with H. It suggests that $Sq_0(Y)$ could be primarily influenced by the plasma drift electric field and controlled by geomagnetic vertical component Z. On the other hand, although the South American station PIL located at the similar geomagnetic latitude (21.4°S) with the African station TAN (23.7°S) and the Australian station KDU (22.1°S), $Sq_0(Y)$ in PIL during solar maximum (52.2 nT) are much weaker than that in TAN (63.2 nT) and KDU (63.3 nT). It is worth noting that the Sq(Y) in South American sector stations is strongly affected by South Atlantic Ocean anomaly. The geomagnetic vertical component *Z* in PIL (~11900 nT) is much weaker than that in TAN (~27500 nT) and KDU (~30100 nT). In consequence, the longitudinal inequality of the yearly average (Sq_0(Y)) might be influenced by the geomagnetic vertical component of the non-dipole field.

The annual variation (Sq_1(Y)) also shows a close relation with the non-dipole geomagnetic anomaly. Sq_1(Y) is quite weak around the South Atlantic Ocean anomaly and fairly strong around the Eurasia and Australia anomaly during both solar maxima and minima years. Other than Sq_0(Y), Sq_1(Y) significantly correlate with *H* in both hemispheres. The correlation coefficients between Sq_1(Y) and *H* are 0.68/0.80 in the northern/southern hemisphere during solar maximum, whereas only 0.11/0.13 between Sq_1(Y) and *Z*.

In response to the annual change of the insolation and E-region ionization, the local ionospheric conductivity enhances during local summer and weakens during local winter. Hence, Yamazaki et al. [2009] inferred that the annual variation of the ionospheric conductivity possibly resulted in the maximum ionospheric current intensity during local summer and the minimum during local winter. In consideration of the negative correlation between the geomagnetic field intensity and the conductivity, the enhancement of *H* could attenuate the annual amplitude of the conductivity and the ionospheric current intensity, leading to the decrease of Sq_1(Y).

However, as shown in **Figures 7c** and **7d**, $Sq_1(Y)$ shows a positive correlation with *H*. This is inconsistent with the conductivity mechanism stated above. In recent studies, Takeda [2013a] proposed that the seasonal variation of Sq(Y) is affected by inter-hemispheric field-aligned currents (IHFACs). These IHFACs are driven by the imbalance of the Sq dynamo action, flowing from the summer to winter hemisphere in the dawn sector and in the reverse direction in the noon sector [Yamashita and Iyemori, 2002, Tomas et al., 2009, Park et al, 2011]. In the circumstance of the IHFACs, Sq(Y) enhances in the summer hemisphere and diminishes in the opposite hemisphere [Takeda, 2013a]. Because of high electric conductivity along the magnetic field lines in the magnetosphere, the IHFAC is primarily determined by the electric potential difference between the geomagnetic north-south conjugate-pair points [Fukushima, 1979]. In other words, the annual change of inter-hemispheric difference of the electric potential, which is produced by the interaction of the geomagnetic horizontal field and neutral wind, plays an important role in the annual variation ($Sq_1(Y)$).

It is widely accepted that the neutral wind blowing in summer is stronger than that in winter, thus the asymmetry of the neutral wind in solstices could cause the electric potential difference between the hemispheres. As the geomagnetic field at the ionospheric footprints of a magnetic line becomes stronger, the electric potential difference could be larger. This is in agreement with the positive correlation between $Sq_1(Y)$ and *H*, suggesting that *H* might strongly influence the IHFACs. In fact, $Sq_1(Y)$ in the South American station PIL (7.8 nT) is very weak compared to the Australian station KDU (9.6 nT) during solar active period, where *H* in PIL and KDU are ~22000 nT and ~35000 nT respectively. Sq$_1$(Y) in African stations, such as HER (6.0 nT), TSU (3.1 nT) and TAN (5.3 nT), are all fairly weak as well, where *H* also remarkably diminishes due to SAO and AFR. Hence, the longitudinal difference of Sq$_1$(Y) might be primarily affected by the IHFACs and the geomagnetic horizontal component.

The semiannual component Sq$_2$(Y) shows distinct features with the above two components. As shown in **Figure 8**, Sq$_2$(Y) is very weak (about 2 nT) during solar minima for most northern hemispheric stations, and becomes a little stronger during solar maximum for some higher latitudinal stations. In contrast, Sq$_2$(Y) in the southern hemisphere significantly correlates with the geographic latitude regardless of the solar activity, and Sq$_2$(Y) in the higher latitude is obviously intense. These features are consistent with the results using a magnetometer chain [Yamazaki et al, 2011]. Since the diurnal tide in the middle latitude atmosphere shows obvious peaks at the equinoxes, identified by ground radar and satellite data, Sq$_2$(Y) might be caused by the semiannual variation of the tidal wind [Yamazaki et al., 2009; Pedatella, 2011].

In the southern hemisphere, Sq$_2$(Y) shows an obviously negative correlation with the horizontal component *H*. In particular, as *H* at four African stations (HER, HBK, TSU and TAN) increases (~12000, ~13000, ~16000 and ~20000 nT) , Sq$_2$(Y) decreases in turn (6.7, 6.4, 6.0 and 4.7 nT in solar maximum years). Considering the negative correlation between *H* and the conductivity, the semiannual amplitude of Sq(Y) might be affected by the ionospheric conductivity and *H*. On the other side, Sq$_2$(Y) is not related to the geomagnetic vertical component Z, implying that Sq$_2$(Y) is independent on the convection electric field.

In summary, the seasonal variations of Sq(Y) at mid-low latitudes is investigated in the present study. The annual variation (Sq$_1$(Y)) is very weak around South Atlantic geomagnetic anomaly region and fairly strong around the Eurasia and Australia anomaly during both solar maxima and minima years. Sq$_0$(Y) and Sq$_1$(Y) correlate well with the geomagnetic component Z and H respectively. In addition, the semiannual variation (Sq$_2$(Y)) in the southern hemisphere is prominent and shows a strong dependence on the geographic latitude and the geomagnetic component H.

Acknowledgements

The authors acknowledge the World Data Center for Geomagnetism, Edinburgh (http://www.wdc.bgs.ac.uk/catalog/master.html) and the observatories that provided data used in the present study. The sunspot number data were obtained from WDC-SILSO, Royal Observatory of Belgium, Brussels (http://sidc.be/silso/home/). This work is supported by the Strategic Priority Research Program of Chinese Academy of Sciences (Grant No. XDB41010304) and the National Natural Science Foundation of China (41874080, 41674168, 41874197).

References

Banks, R. G. and E. C. Bullard (1966), The annual and 27 day magnetic variations, Earth Planet. Sci. Lett., 1(3), 118-120

Bhargava, B. N. (1972), Semiannual and annual modulation of the magnetic field, Planet. Space Sci., 20, 423-427

Briggs, B. H. (1984), The variability of ionospheric dynamo currents, J. Atmos. Sol. Terr. Phys., 46, 419-429

Campbell, W. H. (1982), Annual and semiannual changes of the quiet daily variations (Sq) in the geomagnetic field at North American locations, J. Geophys. Res.,

87(A2), 785-796, doi: 10.1029/JA087iA02P00785
Campbell, W. H. (1989), The regular geomagnetic-field variations during quiet solar conditions, in Geomagnetism, 3, edited by J. Jacobs, chap. 6, pp.386-460, Academic, San Diego, Calif.
Campbell, W. H. and S. Matsushita (1982), Sq currents: A comparison of quiet and active year behavior, J. Geophys. Res., 87(A7), 5305-5308
Chapman, S., and J. Bartels (1940), Geomagnetism, Oxford Univ. Press, London.
Chapman, S., J. C. Gupta, and S. R. C. Malin (1971), The sunspot cycle influence on solar and lunar daily geomagnetic variations, Proc. R. Soc. London Ser. A., 324, 1-15
Chen, G. X., et al. (2007) Statistical characteristics of the day-to-day variability in the geomagnetic Sq field, J. Geophys. Res., 112, A06320, doi:10.1029/2006JA012059
Currie, R. G. (1966), The geomagnetic spectrum-40 days to 5.5 years, J. Geophys. Res., 71(19), 4579-4998
Forbes, J. M. And R. S. Lindzen (1976), Atmospheric solar tides and their electrodynamic effect - I. The global Sq current system, J. Atmos. Terr. Phys., 38, 897-910
Fukushima, N. (1979), Electric potential difference between conjugate points in middle latitudes caused in the ionosphere, J. Geomagn. Geoelectr., 31, 401-409
Hasegawa, M. (1960), On the position of the focus of the geomagnetic Sq current system, J. Geophys. Res., 65, 1437-1447
Hibberd, F. H. (1985), The geomagnetic Sq variation - annual, semiannual and solar cycle variations and ring current effects, J. Atmos. Terr. Phys., 47, 341-352
Le Sager, P. and T. S. Huang (2002), Longitudinal dependence of the daily geomagnetic variation during quiet time, J. Geophys. Res., 107(A11), 1397, doi: 10.1029/2002JA009287
Matsushita, S. (1967), Solar quiet and lunar daily variation fields, in Physics of Geomagnetic Phenomena, edited by S. Matsushita and W. Campbell, chap. II-1, pp. 301-424, Academic, New York.
Matsushita, S. and H. Maeda (1965), On the geomagnetic solar quiet daily variation field during IGY, J. Geophys. Res., 70(11), 2538-2558
Park, J., H. Luhr, and K. W. Min (2011), Climatology of the inter-hemispheric field-aligned current system in the equatorial ionosphere as observed by CHAMP, Ann. Geophys, 29, 573-582
Pedatella, N. M., J. M. Forbes and A. D. Richmond (2011), Seasonal and longitudinal variations of the solar quiet (Sq) current system during solar minimum determined by CHAMP satellite magnetic field observations, J. Geophys. Res., 116, A04317, doi: 10.1029/2010JA016289
Rastogi, R. G. and K. N. Iyer (1976), Quiet day variation of geomagnetic H-field at low latitudes, J. Geomagn. Geoelectr., 28, 461-479
Richmond, A. D. (1979), Ionospheric wind dynamo theory, J.Geomagn. Geoelec., 31, 287-310
Stening, R. J. (1971), Longitude and seasonal variations of the Sq current system,

Radio Sci., 6, 133-137

Stening, R. J. (1977), Field-aligned currents driven by the ionospheric dynamo, J. Atmos. Terr. Phys., 39(8), 933-937

Stening, R. J. (1995), Variations in the strength of the Sq current system, Ann. Geophys., 13, 627-632

Stening, R., T. Reztsovo and L. H. Minh (2005), Day-to-day changes in the latitudes of the foci of the Sq current system and their relation to equatorial electrojet strength, J. Geophys. Res., 110, A10308, doi: 10.1029/2005JA011219

Stening, R., T.Reztsova, and L. H. Minh (2007), Variation of Sq focus latitudes in the Australian/Pacific region during a quiet sun year, J. Atmos. Sol. Terr. Phys., 69, 734-740

Takeda, M. (1996), Effects of the strength of the geomagnetic main field strength on the dynamo action in the ionosphere, J. Geophys. Res., 101(A4), 7875-7880, doi: 10.1029/95JA03807

Takeda, M. (1999), Time variation of global geomagnetic Sq field in 1964 and 1980, J. Atmos. Terr. Phys., 61, 765-774

Takeda, M. (2002a), Features of global geomagnetic Sq field from 1980 to 1990, J. Geophys. Res., 107(A9), 1252, doi: 10.1029/2001JA009210

Takeda, M. (2002b), The correlation between the variation in ionospheric conductivity and that of the geomagnetic Sq field, J. Atmos. Terr. Phys., 64(15), 1617-1621

Takeda, M. (2013a), Difference in seasonal and long-term variations in geomagnetic Sq fields between geomagnetic Y and Z components, J. Geophys. Res., 118, 1-5, doi: 10.1002/jgra.50128

Takeda, M. (2013b), Contribution of wind, conductivity, and geomagnetic main field to the variation in the geomagnetic Sq field, J. Geophys. Res., 118, 4516-4522, doi: 10.1002/jgra.50386

Takeda, M., T. Iyemori and A. Saito (2003), Relationship between electric field and currents in the ionosphere and the geomagnetic Sq field, J. Geophys. Res., 108(A5), 1183, doi: 10.1029/2002JA009659

Takeda, M., Y. Yamada, and T. Araki (1986), Simulation of ionospheric currents and geomagnetic field variations of Sq for different solar activity, J. Atmos. Sol. Terr. Phys., 48, 277-287

Tarpley, J. D. (1973), seasonal movement of the Sq current foci and related effects in the equatorial electrojet, J. Atmos. Terr. Phys., 35, 1063-1071

Tomas, A. T., H. Luhr and M. Rother (2009), Mid-latitude solar eclipses and their influence on ionospheric current system, Ann. Geophys, 27, 4449-4461

Wagner, C. U. (1969), The 'semi-annual' variation of the solar daily quiet geomagnetic variation in the European region, Gerlands Beitr. Geophys., 78, 120-130

Wagner, C. U., D. Mohlmann, and K. Schafer (1980), Large-scale electric fields and currents and related geomagnetic variations in the quiet plasmasphere, Space Sci. Rev. , 26, 391-446

Xu, W. Y. and C. Y. Bai (2009), Role of the African magnetic anomaly in controlling the magnetic configuration and its secular variation, Chinese J. Geophys. (in

Chinese), 52(8), 1985-1992
Yamashita, S. and T. Iyemori (2002), Seasonal and local time dependences of the interhemispheric field-aligned currents deduced from the Orsted satellite and the ground geomagnetic observations, J. Geophys. Res., 107(A11), 1372, doi: 10.1029/2002JA009414
Yamazaki, Y. et al. (2009), Equivalent current systems for the annual and semiannual Sq variations observed along the 210°MM CPMN stations, J. Geophys. Res., 114, A12320, doi: 10.1029/2009JA014638
Yamazaki, Y., et al. (2011), An empirical model of the quiet daily geomagnetic field variation, J. Geophys. Res., 116, A1031, doi: 10.1029/2011JA016487
Yamazaki, Y., and A. Maute (2017), Sq and EEJ-A review on the daily variation of geomagnetic field caused by ionospheric dynamo currents, Space Sci Rev, 206, 299-405, doi: 10.1007/s11214-016-0282-z.

Figures Caption

Figure 1 Geographical distribution of the observatories used in this work. The background is the contour for the vertical component *Z* of the geomagnetic non-dipole field in 2000. Five large-scale anomalies are marked as SAO (the South Atlantic Ocean anomaly), AFR (Africa anomaly), ERA (Eurasia anomaly), AST (Australia anomaly), and NAM (North America anomaly).

Figure 2 Correlation of Sq(Y) at Kanoya (KNY) and sunspot number (SSN) in each month. One dot denotes the monthly mean value in the given month of one year from 1954 to 2010 at each subpanel. The linear regression line is plotted and the regression coefficient is shown at top right corner of each subpanel. The long-term variation of the annual SSN is shown in the bottom panel. Red and blue dots represent high and low solar activity, respectively.

Figure 3 Seasonal variation of Sq(Y) at typical stations in the Northern (a, c, e) and Southern (b, d, f) hemispheres. Months in the local summer are placed at the center for convenient comparison. Error bars represent the standard deviation. Red triangles and blue diamonds represent high and low solar activity years used in this study, respectively.

Figure 4 Annual and semiannual components of Sq(Y) for mid-latitude stations in northern and southern hemispheres. The solid and dotted lines represent the low and high solar activity, respectively.

Figure 5 Annual and semiannual components of Sq(Y) for typical stations in Asia-Australia and Europe-Africa sectors. The solid and dotted lines represent the low and high solar activity, respectively.

Fig.6 Correlation between Sq$_0$(Y) and the geographic latitude, the geomagnetic horizontal component *H* and vertical component *Z* in the northern (a, c, e) and southern (b, d ,f) hemispheres. Linear regression lines are drawn in each panel. Red triangles and blue diamonds represent data in high and low solar activity, respectively.

Figure 7 Same as in Figure 5, but for $Sq_1(Y)$.

Figure 8 Same as in Figure 5, but for $Sq_2(Y)$.

Figures

Figure 1

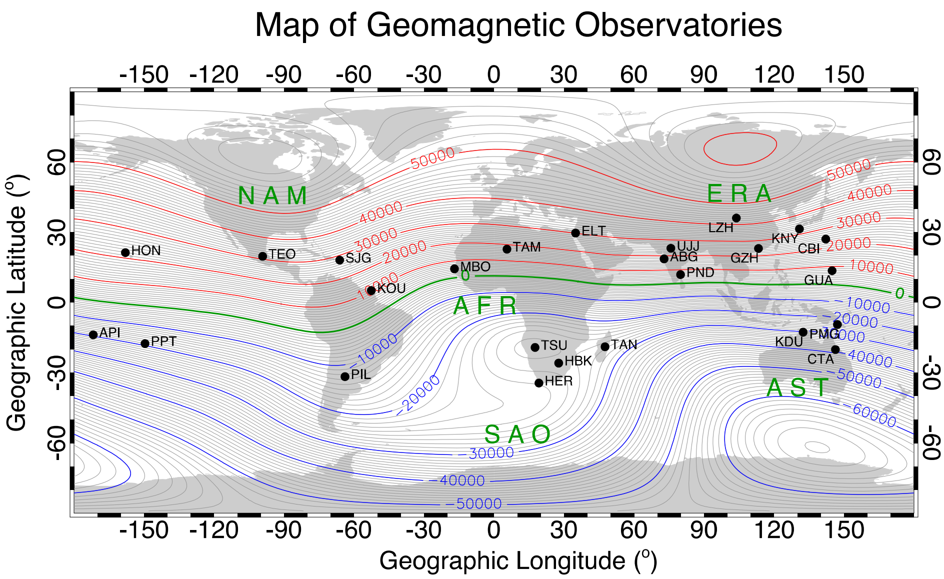

Figure 2

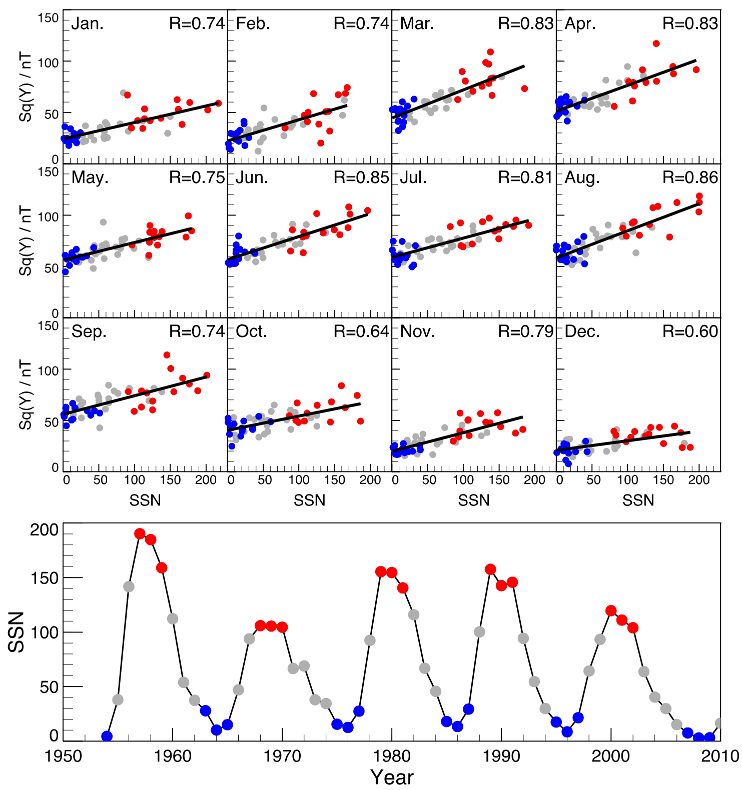

Jan.
R=0.74
Feb.
R=0.74
Mar.
R=0.83
Apr.
R=0.83
May.
R=0.75
Jun.
R=0.85
Jul.
R=0.81
Aug.
R=0.86
Sep.
R=0.74
Oct.
R=0.64
Nov.
R=0.79
Dec.
R=0.60
Sq(Y) / nT
SSN
Year

Figure 3

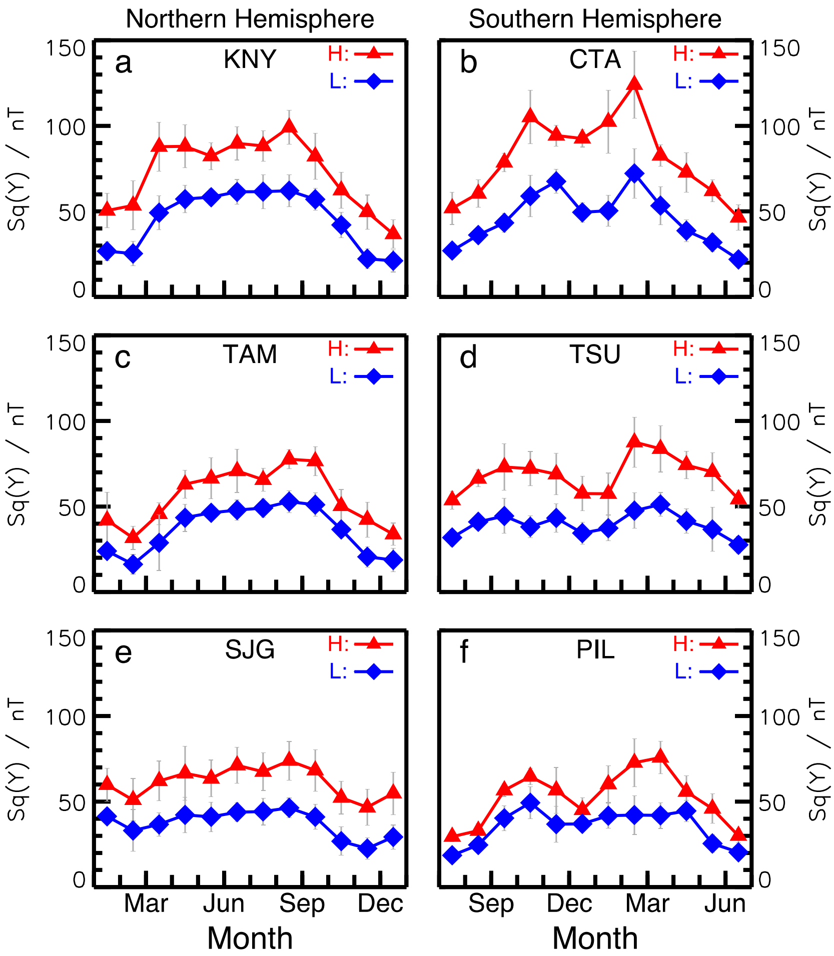

Northern Hemisphere
Southern Hemisphere
a
KNY
b
CTA
c
TAM
d
TSU
e
SJG
f
PIL
H:
L:
Sq(Y) / nT
0
50
100
150
Mar
Jun
Sep
Dec
Sep
Dec
Mar
Jun
Month
Month

Figure 4

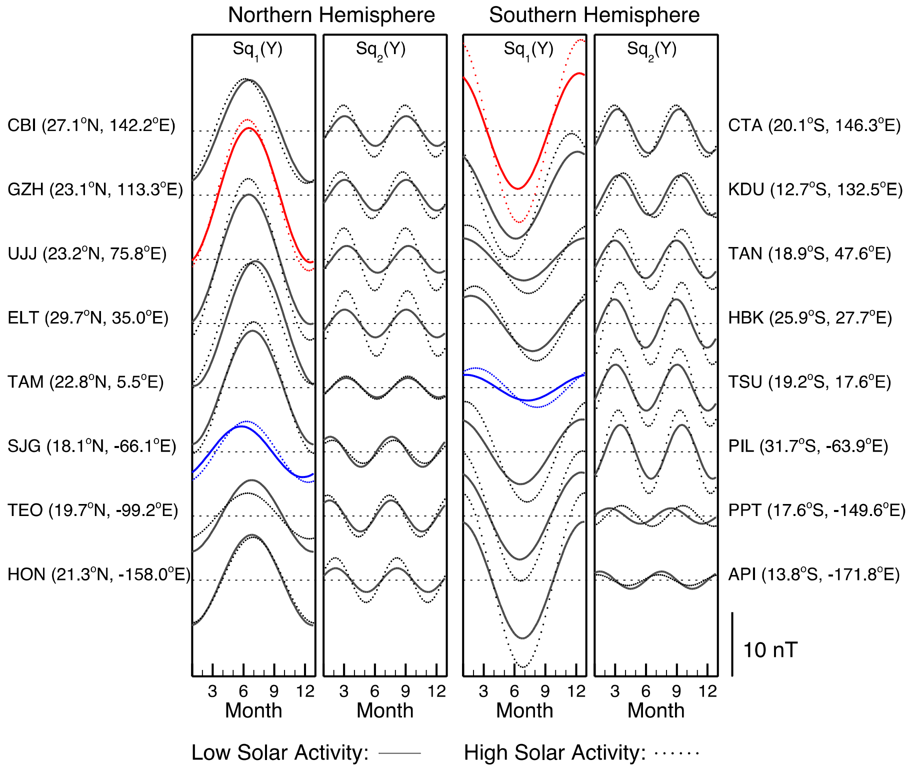

Northern Hemisphere
Southern Hemisphere
Sq$_1$(Y)
Sq$_2$(Y)
Sq$_1$(Y)
Sq$_2$(Y)
CBI (27.1°N, 142.2°E)
GZH (23.1°N, 113.3°E)
UJJ (23.2°N, 75.8°E)
ELT (29.7°N, 35.0°E)
TAM (22.8°N, 5.5°E)
SJG (18.1°N, -66.1°E)
TEO (19.7°N, -99.2°E)
HON (21.3°N, -158.0°E)
CTA (20.1°S, 146.3°E)
KDU (12.7°S, 132.5°E)
TAN (18.9°S, 47.6°E)
HBK (25.9°S, 27.7°E)
TSU (19.2°S, 17.6°E)
PIL (31.7°S, -63.9°E)
PPT (17.6°S, -149.6°E)
API (13.8°S, -171.8°E)
10 nT
3 6 9 12
Month
Low Solar Activity:
High Solar Activity:

531 **Figure 5**

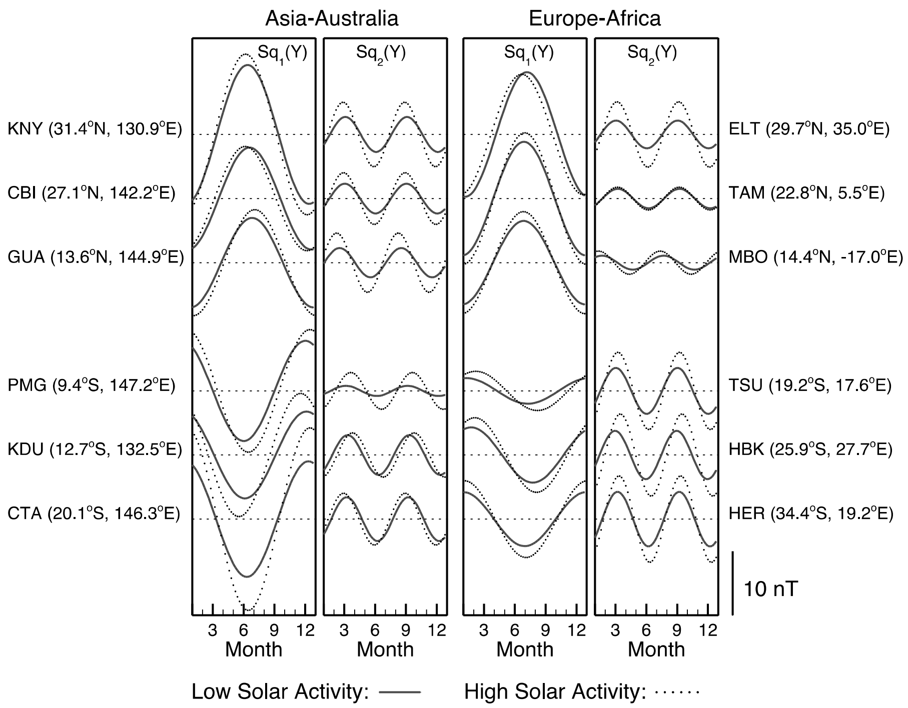

532

533

534

Figure. 6

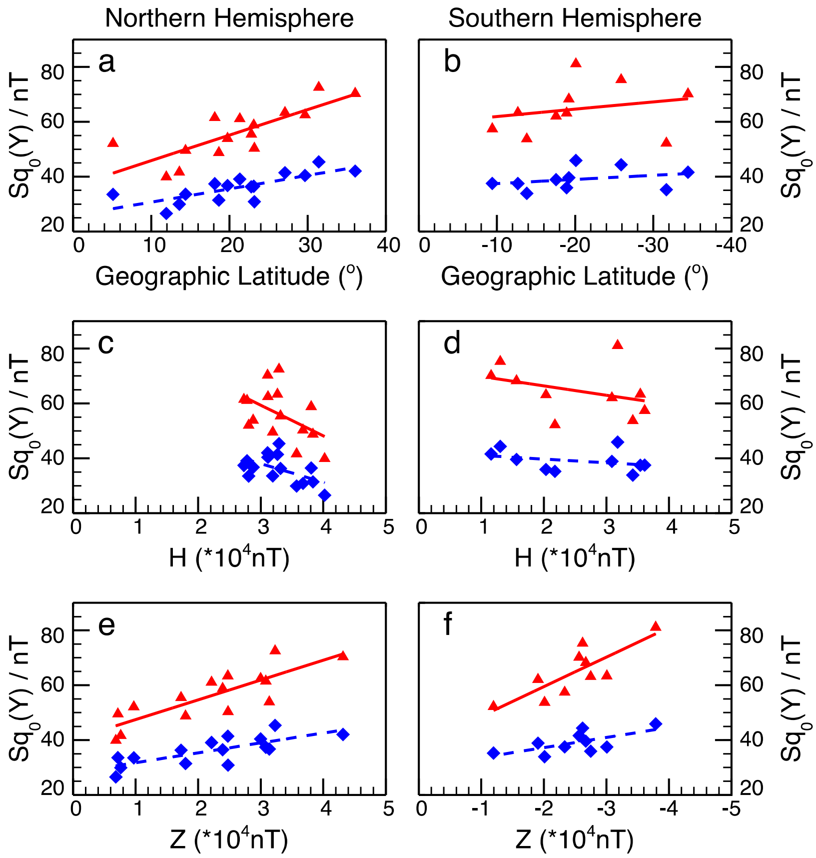
Northern Hemisphere
Southern Hemisphere
a
b
c
d
e
f
$Sq_0(Y)$ / nT
Geographic Latitude (°)
H (*10^{4}nT)
Z (*10^{4}nT)

Figure7

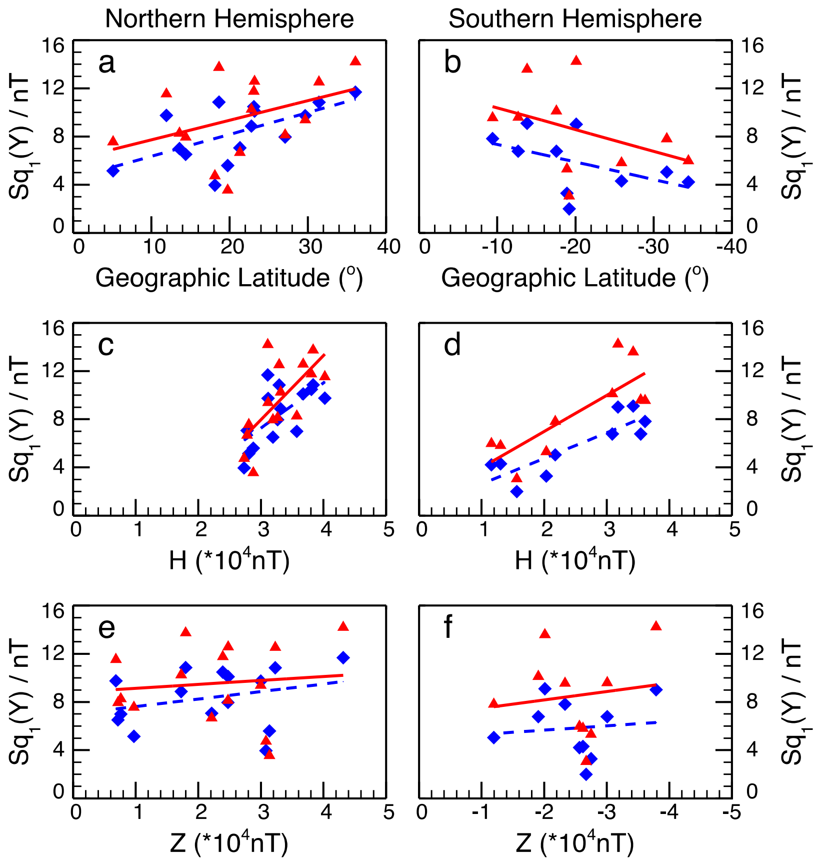

Northern Hemisphere
Southern Hemisphere
a
b
c
d
e
f
Sq1(Y) / nT
Geographic Latitude (°)
H (*10⁴nT)
Z (*10⁴nT)

Figure 8

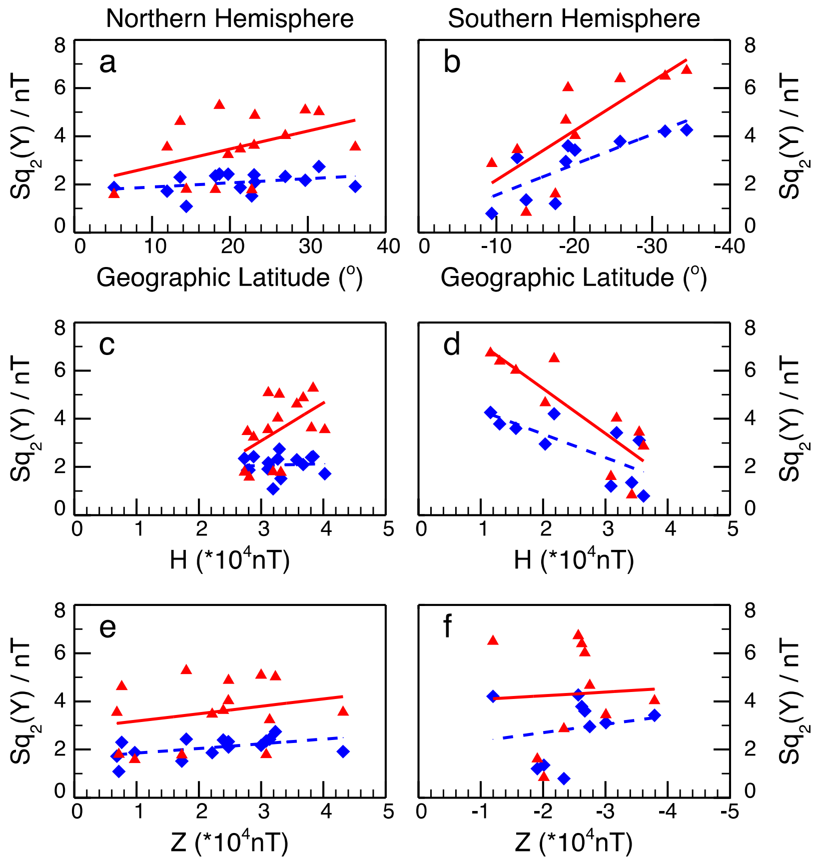
Northern Hemisphere
Southern Hemisphere
a
b
c
d
e
f
Sq2(Y) / nT
Geographic Latitude (o)
H (*10^4nT)
Z (*10^4nT)

Table 1 List of the stations used in this study

Station	Code	GLat. (deg)	GLon. (deg)	GMLat. (deg)	GMLon. (deg)	Years
Hermanus	HER	-34.4	19.2	-33.9	83.7	57
Pilar	PIL	-31.7	-63.9	-21.4	7.0	22
Hartebeesthoek	HBK	-25.9	27.7	-27.1	94.1	39
Charters Towers	CTA	-20.1	146.3	-28.2	220.8	21
Tsumeb	TSU	-19.2	17.6	-18.7	85.6	43
Antananarivo	TAN	-18.9	47.6	-23.7	115.5	41
Pamatai	PPT	-17.6	-149.6	-15.1	285.0	43
Apia	API	-13.8	-171.8	-15.4	262.5	53
Kakadu	KDU	-12.7	132.5	-22.1	205.4	16
Port Moresby	PMG	-9.4	147.2	-17.4	220.3	34
Kourou	KOU	5.1	-52.6	14.9	19.6	15
Pondicherry	PND	11.9	79.9	2.8	152.1	15
Guam	GUA	13.6	144.9	5.2	215.4	54
MBour	MBO	14.4	-17.0	20.2	57.3	57
San Juan	SJG	18.1	-66.2	28.5	5.9	56
Alibag	ABG	18.6	72.9	10.1	146.0	57
Teoloyucan	TEO	19.8	-99.2	28.9	330.1	21
Honolulu	HON	21.3	-158.0	21.6	269.5	57
Tamanrasset	TAM	22.8	5.5	24.7	81.6	21
Guangzhou	GZH	23.1	113.3	12.7	184.6	41
Ujjain	UJJ	23.2	75.8	14.3	149.2	24
Chichijima	CBI	27.1	142.2	18.3	211.4	20
Eilat	ELT	29.7	35.0	26.3	111.8	13
Kanoya	KNY	31.4	130.9	21.8	200.5	53
Lanzhou	LZH	36.1	103.9	25.7	175.9	21

Note: Glat. and Glon. denote the geographic latitude and longitude. GMLat. and GMLon. denote the geomagnetic latitude and longitude. The column "Years" represents the time span of available data provided by each station.

Table 2 Correlation coefficients between Sq(Y) and the geographic latitude and components of the geomagnetic field

	Solar Activity	GLat.	H	Z	-GLat.	H	-Z
		Northern Hemisphere, n=15			Southern Hemisphere, n=10		
$Sq_0(Y)$	L	**0.76**	**-0.54**	**0.76**	0.31	-0.33	**0.65**
	H	**0.79**	-0.49	**0.83**	0.23	-0.36	**0.81**
$Sq_1(Y)$	L	**0.61**	**0.65**	0.28	-0.48	**0.85**	0.10
	H	0.41	**0.68**	0.11	-0.40	**0.80**	0.13
$Sq_2(Y)$	L	0.33	0.07	0.49	**0.79**	**-0.73**	0.19
	H	0.46	0.50	0.25	**0.78**	**-0.85**	0.05

Note: Glat. denotes the geographic latitude. *H* and *Z* denote the horizontal and vertical components of the geomagnetic field. Data satisfying the regression coefficient significance test ($R=0.514$, $p<0.05$ for the northern hemisphere and $R = 0.632$, $p < 0.05$ for the southern hemisphere) are marked in bold.